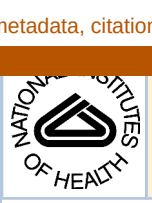

Published in final edited form as:
Ophthalmology. 2009 October ; 116(10): 1960–1970. doi:10.1016/j.ophtha.2009.03.034.

Assessment of Artifacts and Reproducibility across Spectral and Time Domain Optical Coherence Tomography Devices

Joseph Ho, B.S., B.A.[1,2], **Alan C. Sull, B.A.**[1,3], **Laurel N. Vuong, B.S.**[1], **Yueli Chen, Ph.D.**[4], **Jonathan Liu, M.S.**[4], **James G. Fujimoto, Ph.D.**[4], **Joel S. Schuman, M.D.**[5], and **Jay S. Duker, M.D.**[1]

[1] New England Eye Center, Tufts Medical Center, Boston, Massachusetts, USA

[2] Boston University School of Medicine, Boston, Massachusetts, USA

[3] University of Arkansas for Medical Sciences, Little Rock, Arkansas, USA

[4] Department of Electrical Engineering and Computer Science and Research Laboratory of Electronics, Massachusetts Institute of Technology, Cambridge, Massachusetts, USA

[5] University of Pittsburgh Medical Center Eye Center, Eye and Ear Institute, Pittsburgh, Pennsylvania, USA

Abstract

PURPOSE—To report the frequency of optical coherence tomography (OCT) scan artifacts and compare macular thickness measurements, inter-scan reproducibility and inter-device agreeability across three spectral / Fourier domain (SD) OCTs (Cirrus HD-OCT, RTVue-100 and Topcon 3D-OCT 1000) and one time domain (TD) OCT (Stratus OCT).

DESIGN—Prospective, non-comparative, non-interventional case series.

PARTICIPANTS—52 patients seen at New England Eye Center, Tufts Medical Center retina service between February and August 2008.

METHODS—Two scans were performed for each of the SD-OCT protocols: Cirrus macular cube 512×128, RTVue (E)MM5 and MM6, Topcon 3D macular and radial, in addition to one TD-OCT scan via Stratus macular thickness protocol. Scans were inspected for six types of OCT scan artifacts and analyzed. Inter-scan reproducibility and inter-device agreeability were assessed by intraclass correlation coefficients (ICCs) and Bland-Altman plots, respectively.

MAIN OUTCOME MEASURE—OCT image artifacts, Macular thickness, Reproducibility, Agreeability.

RESULTS—TD-OCT scans contained a significantly higher percentage of clinically significant improper central foveal thickness (IFT) post-manual correction (greater than or equal to 11 μm

Corresponding Author/ Reprints Jay S. Duker, MD Department of Ophthalmology, Chairman Tufts Medical Center 800 Washington St., Box #450, Boston, MA, 02111 Tel: 617−636−4677; Fax: 617−636−4866 E-mail: JDuker@tuftsmedicalcenter.org.

Meeting Presentation
Abstract accepted for poster presentation at Association for Research in Vision and Ophthalmology Annual Conference, May 2009, Fort Lauderdale, FL.

change) compared to SD-OCT scans. Cirrus HD-OCT had a significantly lower percentage of clinically significant IFT (11.1%) compared to the other SD-OCT devices (Topcon 3D: 20.4%, Topcon Radial: 29.6%, RTVue (E)MM5: 42.6%, RTVue MM6: 24.1%; p= 0.001). All three SD-OCT had central foveal subfield thicknesses significantly greater than TD-OCT post manual correction (p< 0.0001). All 3 SD-OCT demonstrated a high degree of reproducibility in the central foveal region (ICC= 0.92 to 0.97). Bland-Altman plots showed low agreeability between TD- and SD-OCT scans.

CONCLUSIONS—Cirrus HD-OCT scans exhibited the lowest occurrence of any artifacts (68.5%), IFT (40.7%) and clinically significant IFT (11.1%) compared to all other OCT devices examined, while Stratus OCT scans exhibited the highest occurrence of clinically significant IFT compared to all 3 SD-OCT examined. Significant differences in macular thickness occurred among SD- and TD-OCT. All SD-OCT examined revealed high reproducibility in the central foveal subfield (ICC 0.92 to 0.97). Higher scan density and speed obtainable with SD-OCT appear to improve reproducibility. Although software breakdown occurred to a variable degree with different commercial OCT, further work on improving segmentation algorithm to decrease artifacts is warranted.

Introduction

Optical coherence tomography (OCT)[1] is a non-invasive imaging technique clinically utilized for the visualization of the retina, optic nerve, and anterior segment.[2-4] Conventional time domain OCT employ a mechanically scanning reference arm and sequentially measure the echo time delays.[5] In contrast, the newer generation spectral or Fourier domain OCT use a stationary reference arm to obtain an interference spectrum, which then undergoes Fourier transformation to allow for simultaneous measurement of all the echo time delays of light.[6] As a result, this new technology significantly improves the system speed and sensitivity.[7-9] Spectral / Fourier domain OCT have an image acquisition speed of 18,000 to 50,000 A-scans per second, with a maximum of approximately 300,000 A-scans per second[10, 11], limited by signal levels, as compared to time domain maximum of approximately 400 A-scans per second. The faster imaging time translates into decreased motion artifacts and greater coverage of the retina. The axial resolution of an OCT device is inversely proportional to the bandwidth of its light source.[12] Standard time domain OCT utilizes a low-coherence superluminescent diode (SLD) light source at a wavelength of 840 nm and a bandwidth of ~25 nm, allowing it to achieve an 8−10 μm axial resolution. In contrast, most commercially available spectral / Fourier domain OCT devices use an SLD light source with a bandwidth of ~50 nm, achieving a 5−8 μm axial resolution in tissue. The greater resolving power of these OCT devices translates into enhanced capabilities to observe fine ocular pathologies.

The current clinical uses of OCT in retina has largely been qualitative, for the visualization of pathologies such as macular edema[13], subretinal fluid[14], epiretinal membranes (ERM)[15-17], vitreomacular traction (VMT)[18-20], macular holes[21, 22], photoreceptor layer and/or retinal pigment epithelium (RPE) disruption[23], and choroidal neovascularization membranes (CNVM)[24, 25]. However, it is now possible to acquire large volumes of quantitative data for OCT analysis with the improved scan density, retinal coverage and image resolution of the spectral domain OCT. Quantitative OCT analysis is playing an increasingly important clinical role with the development of anti-VEGF (Vascular Endothelial Growth Factor) therapies for tracking treatment outcomes in patients with neovascular age-related macular degeneration (AMD). In these patients, treatment success is defined anatomically as a reduction in intra/sub-retinal and sub-RPE fluids, which translates into a reduction in thickening of the Early Treatment Diabetic Retinopathy Study (ETDRS)-like map.[26] Retinal thickness is generated by measuring the distance between the inner retinal border (vitreous/retina interface) and the outer retinal border (retinal/RPE interface). Then retinal thickness are tracked accurately over time via generation of OCT enface images and registering various landmarks (i.e. blood vessels)

onto a fundus image generated at baseline. The reliability of such change analysis depends on the accuracy of segmentation software. While much progress has been made in improving the accuracy of segmentation, segmentation software breakdown still occur with both time domain and spectral / Fourier domain OCT devices.[27-31] Other OCT artifacts which hinder the accuracy of thickness analysis may be the result of operator-induced acquisition errors, such as the shifting of OCT images out of the range of the scan area. Additionally, OCT artifacts may result from patient motion or eccentric fixation. While segmentation software breakdown may be manually corrected, it is time consuming, not always practical, and sometimes not feasible in clinical settings.

This study utilized scans from three commercially available spectral / Fourier domain OCT instruments and one standard time domain OCT device to evaluate six different types of OCT scan artifacts in eyes with macular disease. This study also assessed inter-scan reproducibility and time domain to spectral domain OCT agreeability in pathological states.

Methods

Subjects

Patients seen at the New England Eye Center, Tufts Medical Center between February and August 2008 who fit the inclusion criteria were invited into this study. Qualified patients were then enrolled into the study after receiving their informed consent. The study was conducted in accordance with the ethical standards stated in the 1964 Declaration of Helsinki and approved by the Institutional Review Board of Tufts Medical Center. Ocular pathologies of eyes in this study included lamellar or full-thickness macular holes, neovascular and non-neovascular AMD, posterior vitreous detachment, CNVM, idiopathic juxtafoveal telangiectasia (IJT), diabetic retinopathy, retinal vascular obstruction, Stargardt disease, ERM, cystoid macular edema, central serous chorioretinopathy (CSCR), and angioid streaks.

Technology Utilized

In patients with bilateral disease, the eye that was most seriously affected, based on Snellen visual acuity, was selected as the study eye. Subjects were scanned on a single time domain OCT device: Stratus OCT (software version 4.0; Carl Zeiss Meditec, Inc., Dublin, CA, USA), and three spectral / Fourier domain OCT: Cirrus HD-OCT (software version 3.0; Carl Zeiss Meditec, Inc., Dublin, CA, USA), RTVue-100 (software version 3.5; Optovue, Inc., Fremont, CA, USA) and Topcon 3D OCT-1000 (software version 2.12; Topcon, Inc., Paramus, NJ, USA). Subjects were scanned twice on each of the three spectral / Fourier domain devices with each protocol, having one minute rest between scans (in this study, the term “scan”, if not otherwise specified, is defined as all images acquired within a given protocol; for example, all 128 raster scans in the Cirrus macular cube 512×128). Scans were obtained on the same day, by the same operator, and in variable sequence.

The Cirrus HD-OCT has a 5 μm axial image resolution and an imaging speed of 27,000 axial-scans per second. The RTVue-100 has a 6 μm axial image resolution and a speed of 26,000 A-scans per second. Topcon 3D-OCT 1000 has a 5 μm axial image resolution and a speed of 18,000 A-scans per second. The Stratus OCT has a 8−10 μm axial resolution and acquires images at speeds of 400 axial scans per second.

Scan Protocols

Patients were scanned via time domain detection using the Stratus OCT and were imaged only once per visit. The macular thickness protocol (6 radial, equally-spaced 6 mm scans with 512 A-scans per line) was performed. All scans acquired had a signal strength of at least 5 (out of 10).

Subjects were scanned via spectral / Fourier domain detection with three different commercial SD- OCTs. Participants were scanned twice with each protocol per visit:

- The Cirrus HD-OCT scan protocol (~2.5 seconds) consisted of the macular cube 512×128 scan (with 128 horizontal raster, 512 A-scans per line, in a 6×6 mm area, resulting in a sample density of ~47 μm between A-scans in the superior-inferior direction and ~12 μm in the temporal-nasal direction). All scans had signal strengths of at least 5 (out of 10).
- The RTVue-100 scan protocol consisted of MM5 (0.78 seconds; outer 5×5 mm grid of 11 horizontal and 11 vertical lines of 668 A-scans each spaced 0.5 mm apart and an inner 3×3 mm grid of 6 horizontal and 6 vertical lines with 400 A-scans each spaced 0.5 mm apart, resulting in the inner 3×3 mm region being sampled with 250 μm between B-scans and 10 μm between A-scans in each B-scan) or EMM5 (0.90 seconds; outer 6×6 mm grid of 13 horizontal and 13 vertical lines with 668 A-scans each and an inner 4×4 mm grid of 8 horizontal and 8 vertical lines with 400 A-scans each, resulting in the inner 4×4 mm region being sampled with 250 μm between B-scans and 10 μm between A-scans in each B-scan) and MM6 (0.27 seconds; 12 radial scans with 1,024 A-scans each, with a 6 mm diameter). All scans had signal strengths of at least 40 (out of 100). Patients imaged from July 2008 onwards were scanned with EMM5 instead of the MM5 due to the availability of this new scan protocol.
- The Topcon 3D-OCT 1000 scan protocols consisted of the radial scan (0.30 seconds; 6 radial scans with 1024 A-scans each) and 3D macular scan (3.6 seconds; 128 raster scans with 512 A-scans each, within a 6×6 mm area, resulting in a sample density of ~47 μm between A-scans in the superior-inferior direction and ~12 μm in the temporal-nasal direction.). All scans had signal strengths of at least 40 (out of 100).

Artifacts Classification

Inner/outer retinal layer misidentification—Each of the 9 subfields of the ETDRS- like map was recorded for all scans taken. The central foveal region was the central 1 mm of the map. Immediately surrounding the central foveal subfield was the parafoveal region, which had a diameter of 3 mm. Surrounding the parafoveal region was the perifoveal region (5 mm diameter).

Subsequently, all images acquired within each scan pattern (for example, 128 raster scans in Cirrus macular cube 512×128) were reviewed to check for segmentation breakdown in the inner and outer retinal layers. All devices used the internal limiting membrane for the placement of the inner retinal layer. For the outer retinal layer: Stratus OCT used the inner segment/ outer segment (IS/OS) junction, Cirrus HD-OCT and the RTVue-100 used the RPE, and the Topcon 3D-OCT 1000 used the photoreceptor outer segment tip. Figure 1 demonstrates the proper placement of the outer retina for all devices analyzed in this study. If segmentation algorithm broke down in the inner retinal layer, it was recorded as **inner retina misidentification**. If segmentation broke down in the outer retinal layer, it was recorded as **outer retina misidentification**.

Inaccurate foveal thickness—In cases where segmentation breakdown occurred in the inner or outer retinal layers within the central foveal region (center 1 mm), manual correction was employed to correct for the segmentation breakdown. Cirrus 512×128 cube scan has a 6×6 mm scan area composed of 128 horizontal B-scans. To determine the number of scans located in the central foveal region, 128 B-scans were divided into 6 mm to obtain ~22 B-scans. Topographic map and OCT B-scans were then used to locate the 22 B-scans centered at the central foveal region. RTVue MM5 scan has a retinal scan area of 5×5 mm and is composed of 17 horizontal B-scans, while the EMM5 has a scan area of 6×6 mm with 21 horizontal B-

scans. A similar approach to the Cirrus was undertaken to obtain a central foveal region of ~4 B-scans for both RTVue scan patterns and then topographic map and OCT B-scans were used to locate these scans in the central foveal regions. Topcon 3D scan protocol allowed for the placement of the EDTRS grid over the topographic map. The central foveal subfield of the EDTRS grid could be moved over the central foveal region shown on the topographic map and B-scans could subsequently be analyzed for segmentation breakdown at the central foveal region.

For spectral / Fourier domain OCT, inner and outer retinal boundary lines were redrawn where errors occurred to reflect their proper locations by one of the authors (JH). For Stratus OCT, since there was no way to redraw segmentation lines, OCT images with improper segmentation line placements were not factored into the retinal thickness calculations and only images with proper segmentation line placements were included. Changes ≥ 1 μm in the average central foveal thickness as reported by the software post-manual correction were recorded as an **inaccurate foveal thickness**, while changes ≥ 11 μm post-manual corrections within the central foveal subfield were recorded as **clinically significant inaccurate foveal thickness**. This clinically significant cutoff point was established from previously reported results of Chan et al who found that the average standard deviation of central macular thickness measurements in normal eyes was 11 μm via a time domain OCT detection.[32] This value also matched the order of the OCT system's axial resolution. Therefore, we selected this value as a conservative estimate for a significance threshold of clinically significant error in foveal thickness, since post-manual changes less than this value may not be great enough to warrant correction clinically, as this variation could occur by chance.

Off-center fixation—An **error in fixation** was recorded when the central foveal subfield of the ETDRS-like map was more than 0.25 mm away from the true center based on both the topographic map and OCT B-scan data. In cases of certain pathologies (for example, neovascular AMD) where foveal centers were not apparent from topographic information alone, visual examinations of all acquired raster scans were utilized to estimate their locations. For RTVue-100 and Topcon 3D-OCT 1000, the ETDRS- like map was moved to where the central foveal region should be based on the topographic map and raster scan images in cases of eccentric fixation.

Out of range—Out of range artifacts were identified when OCT images were vertically shifted, causing a truncated inner or outer retina. Figure 2 presents examples of all the artifact types analyzed in this study.

Statistical Analysis

Mean thickness, standard deviation and 95% confidence interval for each region of the EDTRS-like map were computed and their significance was compared across all devices using repeated measure analysis of variance (ANOVA) [SAS Institute, Cary, NC]. Logs of central foveal thicknesses (CFTs) for first and second scans (both pre- and post manual adjustment) were taken and then two-tailed T-tests [Microsoft Excel, Redmond, WA] were conducted to compare the mean differences between first and second scan CFTs. First scan MM5 and EMM5 CFTs post log-transformation was also compared using two-tailed T test.

The percent occurrence of any errors, improper CFT (≥1 μm and ≥ 11μm), inner and outer retina misidentification, out of range error, and off center errors were computed for the first scan of each device and their significance across all devices was determined by generalized estimating equations [SAS Institute, Cary, NC]. The absolute value of the change in CFT post-manual correction was grouped into increasing breakdown thresholds (from 10 μm to 250 μm) by each device and then counted and plotted (Figure 3) [Microsoft Excel, Redmond, WA].

Additionally, the rate of clinically significant improper foveal thickness occurring in each of the devices was broken down by diagnosis. Subgroup analysis via generalized estimating equations was conducted for diseases that yielded the highest number of patients (ERM and neovascular AMD) in order to compare the relative frequencies of clinically significant inaccurate foveal thickness occurring among the OCT devices. Percentage of inner and outer retina misidentification was also calculated for each of the disease states examined grouped by devices.

Reproducibility of scans was evaluated by computing the intraclass correlation coefficient (ICC) and 95% confidence interval comparing average first versus second scan foveal thickness measurements in all subfields. Bland-Altman plots were constructed to assess the level of agreeability between time domain and each spectral domain OCT device. The Bland-Altman limits of agreement (95% confidence interval) was also computed.

Results

At the end of the recruitment period, a total of 52 patients were enrolled, including two who returned to the clinic one month later for repeat scans. The breakdown of retinal pathologies was as follows: 15 ERM, 13 neovascular AMD, 8 diabetic macular edema and diabetic retinopathy, 6 non-neovascular AMD, 4 VMT, 4 lamellar or full thickness macular holes, 3 cystoid macular edema, 3 CSCR, 2 retinal vascular obstruction, 1 IJT, 1 Stargardt disease, and 1 angioid streaks. The mean age of the subjects was 67 ± 13 years (with a range from 27 to 92). Gender breakdown consisted of 30 females and 22 males, of whom 49 were Caucasian, 2 were African-American and 1 was Middle Eastern.

Macular thickness

Table 1 showed the mean and standard deviation for each of the foveal subfields in both time- and spectral / Fourier domain OCT. Standard deviations were all largest at the central foveal region in both time domain as well as spectral / Fourier domain OCT. Parafoveal regions were the thickest on average compared to central foveal or perifoveal subfields. T-tests comparing MM5 to EMM5 scans for each foveal subfield were performed post log-transformation of data to assess the validity of using the two types of scans interchangeably in analysis. No statistical difference between scans was found (data not shown). Scans from all three spectral domain OCT all generated greater CFT compared to Stratus OCT scans post manual correction. Paired T -tests were conducted after log- transformation of data to compare first versus second scan CFT and neither pre- nor post-manually adjusted data showed statistical significance. This analysis was not conducted for the time domain OCT since no repeat scans were done for this device.

Error rate

Spectral / Fourier domain and time domain OCT both revealed high occurrence of any artifacts (Table 2), ranging from 68.5% (Cirrus cube scan 512×128) to 90.60% (Topcon 3D). The high incidences of errors present in these devices was largely due to our strict definition of improper foveal thickness, where even changes in CFT of 1 μm post-manual adjustment would be categorized as an incidence of this artifact. Thus while the occurrence of improper foveal thickness may be high, changes as small as 1 μm post-manual correction would most likely not be clinically significant, that was why we devised the “clinically significant improper foveal thickness” artifact category.

While spectral / Fourier domain detection (RTVue (E)MM5) had the highest percent of improper foveal thicknesses, time domain OCT had the highest percentage of clinically significant errors (change post- manual correction ≥ 11 μm). Segmentation errors in the inner

retina was universally greater compared to that for the outer retina across both spectral / Fourier domain and time domain OCT. Out of range and off center artifacts were among the lowest in terms of the error incidences. Out of range error was the only artifact category that did not reach statistical significance (p= 0.177) when compared across OCT devices and off center artifact was borderline significant (p= 0.047).

Table 3 presents the percent of clinically significant errors (≥11 μm) for each of the commercial OCT devices broken down by diagnosis. Lamellar/full thickness macular holes caused the highest percentages of significant errors for Stratus OCT, RTVue (E)MM5 and MM6 and Topcon Radial. Retinal vascular obstruction and Stargardt disease caused the greatest percentage of significant error in Cirrus Cube 512×128 and Topcon 3D Macular, respectively. Neither angioid streaks nor IJT caused any level of significant errors. Subgroup analysis for neovascular AMD/CNVM and ERM revealed that Cirrus HD-OCT had the lowest percentages of any type of artifacts for both disease states, although these differences were not statistically significant (data not shown).

The absolute level of error post manual correction for each of the devices was broken down by threshold values and plotted (Figure 3). The Cirrus 512×128 cube scan had the lowest number of errors at a threshold >10 μm, while (E)MM5 had the highest number of errors out of the six measurement protocols at that threshold. Cirrus 512×128 cube scan also had the most rapid drop to the lowest level of error, occurring at an error threshold > 50 μm. Stratus OCT had the second lowest number of errors at a threshold of >10 μm but plateau at the highest count of errors. RTVue ((E)MM5, MM6) and Topcon scans (3D macular, radial) displayed similar behavior in the distribution of errors in each of the breakdown thresholds.

Percentage of inner and outer retina misidentification was calculated for each of the disease states grouped by devices (Table 4). Highest average percentage of outer retina misidentification across all OCT devices occurred in CSCR (84%), cystoid macular edema (64%) and neovascular AMD (60%), while highest average percentage of inner retina misidentification occurred in VMT (95%), ERM (90%) and lamellar/full thickness macular hole (75%).

Agreeability

Results from Bland-Altman plots assessing agreeability of mean central subfield thickness between time domain and the three spectral / Fourier domain OCT were shown in Table 5. Sample plot comparing Cirrus versus Stratus OCT CFT was shown in Figure 4 (remaining plots not shown). The limits of agreement (95% confidence interval) crossed zero for all scans and ranged from 309 μm ((E)MM5) to 396 μm (Topcon radial).

Reproducibility

ICC between first and second scans were computed to assess reproducibility for each spectral / Fourier OCT device (Table 6). All devices demonstrated excellent reproducibility at the central foveal region, with ICCs above 0.92. The parafoveal and perifoveal regions generally had greater variability in the ICCs.

Discussion

Error rate

Several studies have previously reported high levels of errors generated with time domain detection in pathological eyes.[27-30] In our study, we found that Stratus OCT created significantly higher rates of clinically significant errors compared to any of the spectral / Fourier domain OCT. Although Stratus OCT had the highest number of clinically significant errors—

the most important error type examined, it did not perform the poorest out of all of the artifact types analyzed. In fact, Stratus OCT scans had the lowest percentage of outer retina misidentification (p= 0.005). This finding suggested that while spectral domain technology may be superior in terms of decreasing the overall number of clinically significant segmentation errors, differences in technology may not be the only factor in the determination of segmentation breakdown rates. Other factors such as the quality of the segmentation software written for the OCT device may in fact play a very important role in determining the incidences of segmentation errors present for a device. Additionally, it was also surprising that the instances of inner retina misidentification were greater than that for the outer retina, as the former was considered easier and more accurate to segment. A possible explanation for this could be the number of diseases of the vitreo-retinal interface (15 ERM, 4 VMT, 4 lamellar/ full thickness macular hole) present in this study.

Cirrus HD-OCT had the lowest percentage of improper foveal thickness among spectral / Fourier domain and time domain OCT. The shape of its breakdown threshold graph reflected this finding: Cirrus started with the lowest number of clinically significant improper foveal thickness, later dropping down to a minimum point the earliest. Stratus OCT plateau with the highest number of scans with large changes in central foveal thickness. This may be due to the mechanism of correction that was available for this device, such that in cases where multiple scans contain segmentation artifacts, only a few number of scans without errors were used to extrapolate the foveal thickness.

Out of range artifacts, a largely operator induced error, was the only error that did not reach statistical significance. This may suggest that the OCT user interfaces examined in this study were similar in terms of the ease of acquisition. Additionally, operator induced error may not be the major factor causing the disparity in artifact prevalence seen between these devices. Off center fixation was largely a patient induced error. Cirrus HD-OCT scans had the lowest instances of this artifact (p= 0.047). One possible explanation for the low instances of this artifact may be the improved speed decreasing the instances of fixation drift.

The percentage of inner and outer retina misidentification was broken down across the various disease states (Table 4) and the results were as expected: in diseases of the vitreo-retinal interface (such as ERM, VMT, lamellar/full thickness macular hole), the prevalence of inner retina misidentification were high; in diseases where subretinal fluid were present thus obscuring the outer retinal boundary (i.e. neovascular AMD and CSCR), the percentage of outer retinal misidentification were increased.

Reproducibility

Numerous studies confirm the high reproducibility of macular thickness measurements in time domain OCT.[33-37] However, the reproducibility among spectral domain OCT have been less studied. Leung, et al found that SD-OCT macular thickness measurements demonstrated high repeatability with ICC ranging from 0.92 to 0.99 using Topcon 3D OCT-1000 in normal eyes.[38] Forooghian, et al also found high reproducibility for SD-OCT using the Cirrus HD-OCT with ICCs ranging from 0.84 to 1.00 in eyes with clinically significant macular edema.[39] This current study also found high levels of repeatability among spectral domain systems, particularly in the central foveal region with ICCs ranging from 0.92 (Cirrus and RTVue (E) MM5) to 0.97 (Topcon Radial). In addition, we found a wider range of ICCs outside of the central foveal region, most evident perifoveally (where the lowest ICCs could be found across all scans except for the Topcon 3D protocol). One possible explanation for this observation may be the presence of eccentric fixation or out of register error, causing scans to get cut off at the periphery of the scan area, leading to segmentation errors to occur at higher rates in the perifoveal regions. While reproducibility in peripheral regions may be lower compared to the

central foveal region, this may not be as clinically significant, since peripheral vision may not be as significant in central visual acuity measures.

Leung et al suggested that the higher reproducibility observed in spectral / Fourier domain systems compared to those in time domain OCT may be due to the former's higher scan rate, which enabled macular mapping with fewer motion artifacts and thus more accurate and repeatable segmentation. When examining Cirrus macular cube 512×128 versus Topcon 3D scan, this assertion appeared to agree with our data. While both protocols had the same scan density and area, different ranges of repeatability were obtained. Cirrus HD-OCT, with its scanning speed of 27,000 A-scans/second, gave a smaller range in the limits of agreeability or 95% CI (326 μm) and thus higher repeatability. Topcon 3D, with a slower scanning speed of 18,000 A-scans/second, produced a larger range in the limits of agreeability (360 μm). Forooghian et al proposed that higher scan density may also aid in the reproducibility of scans since increased sampling points would decrease the level of extrapolation used between points. Data from Paunescu et al confirmed that high density scanning (512 A-scans/line) led to significantly higher reproducibility compared to low density scans (128 A-scans/line) on Stratus OCT.[33] RTVue MM6 scan pattern consisted of 12 radial scans with 1,024 A-scans/line within a 6 mm diameter circle while Topcon radial scan consisted of 6 radial scans also with the same A-scans/line within the same size circle. Given the specifications, RTVue MM6 had a denser scan pattern compared to Topcon radial scan and the range for the limits of agreement between the two scans did seem to reflect this difference (319 μm for MM6 and 396 μm for Topcon radial). It was unclear in this comparison how much the higher scanning speed of the RTVue over the Topcon contributed to the former's higher reproducibility (as opposed to the increased scan density), but we speculate that both factors played roles in their relative reproducibility.

Although higher density scanning may compromise scanning speed, and vice versa, it appeared that both improved scanning speed as well as increased scanning density may play roles in improving reproducibility of scans in spectral / Fourier domain OCT.

Agreeability

Bland-Altman plots and their limits of agreement (95% confidence interval) were computed to assess agreeability between time domain and each spectral / Fourier systems. The range of agreement was broad, from 309 μm (Stratus OCT versus (E)MM5) to 396 μm (Topcon Radial). With such poor agreement, thickness measurements obtained from time domain systems could not be directly compared to spectral /Fourier domain OCT. Our results were in accordance to Leung and Forooghian, whose largest ranges for limits of agreement were 38.6 μm and 168 μm, respectively. The relative ranges obtained from their papers was not unexpected, as the first study was conducted in normal patients and the latter study in patients with clinically significant diabetic macular edema. The present study was conducted in patients with a wide range of retinal pathologies, which may be the reason why the limits of agreement were even wider. A possible way to improve agreeability and thus increase the direct comparability among commercial OCT devices might be to standardize the boundary of the outer retina to a specific location. In this study, the least amount of outer retinal breakdown occurred with the Stratus OCT, which segmented the outer border at the IS/OS junction and so this may appear to be a location of interest for future development of segmentation software. However, when the level of outer retinal breakdown was separated out by diseases, it increased substantially in diseases where the outer retinal boundary becomes obscured, such as neovascular AMD. In fact, Topcon radial (23% breakdown), Cirrus (54%), and (E)MM5 (60%) scans all performed better compared to Stratus OCT (67%) in segmentation of the outer retina in this example.

Macular Thickness

Like Leung and Forooghian, we also found significantly different macular thickness measurements between time domain and spectral domain systems. Both groups found higher thickness measurements in spectral domain OCT compared to time domain OCT. We also arrived at the same conclusion for post-correction thickness for all three SD- OCT. This was not surprising since the boundary for the outer retina was set at the RPE for Cirrus and RTVue and at the photoreceptor outer segment tip for the Topcon, while the boundary was set at the IS/OS for the Stratus OCT. Since there was no agreement in the macular thicknesses obtained from each of the spectral / Fourier domain devices, future work will need to be conducted to find the normal macular thickness for each device. Doing this may aid in the standardization of macular thicknesses across the various spectral / Fourier domain OCT.

The standard deviation for the central foveal region was larger than in any other regions for all scan protocols, this was likely due to the foveal depression causing greater variability in the distance between the inner and the outer retina.

Limitations

There were several limitations to this study. First, three experienced operators were used to acquire the OCT images (JH, ACS, LNV). Although the spectral / Fourier domain OCT examined in this study all had registration features which may already decrease intra-patient variability, as an additional precaution, the same operator conducted both the first and the repeat scans for each patient. Additionally, a minority of the patients scanned were not dilated. Small pupils may affect scan quality in patients. Patients were scanned only once on the Stratus OCT, as a part of the baseline examination in this group. Thus the reproducibility of Stratus OCT in diseased eyes could not be obtained. Lastly, while this study examined eyes across a broad spectrum of retinal disorders, note that results obtained from this study can only be generalized to this subset of patients. Since some of the disease categories had small number of patients within them, we were not able to compare error rates across the various devices for these pathologies in sub group analysis.

This was the first study, to our knowledge to compare the reproducibility, agreeability, and error rates among the various spectral / Fourier OCT in eyes with a wide range of underlying retinal pathologies. Cirrus HD-OCT scans exhibited the lowest occurrence of any artifacts (68.5%), improper foveal thickness (40.7%; $\geq$ 1 μm change post-manual correction) and clinically significant improper foveal thickness (11.1%; $\geq$ 11 μm change post-manual correction) compared to the other OCT devices examined in this study. Stratus OCT scans exhibited the highest occurrence of clinically significant improper foveal thickness compared to all 3 spectral domain OCT analyzed. All spectral / Fourier domain OCT examined in this study revealed high levels of reproducibility, especially in the central foveal subfield (with ICCs all above 0.92). Significant differences in macular thickness existed between the various spectral / Fourier domain OCT examined and with the Stratus OCT. Higher scan density and speed may improve reproducibility of OCT scans. Although the rates of any artifacts vary across commercial OCT, ranging from 68.5 % (Cirrus 512×128 cube) to 90.6% (Topcon 3D scan), these rates were large enough to warrant improvement in segmentation algorithm to decrease future incidences of these artifacts.

References

1. Huang D, Swanson EA, Lin CP, et al. Optical coherence tomography. Science 1991;254:1178–81. [PubMed: 1957169]
2. Ramos JL, Li Y, Huang D. Clinical and research applications of anterior segment optical coherence tomography - a review. Clin Experiment Ophthalmol. In press

3. Hitzenberger CK, Baumgartner A, Drexler W, Fercher AF. Interferometric measurement of corneal thickness with micrometer precision. Am J Ophthalmol 1994;118:468–76. [PubMed: 7943125]
4. Hee MR, Izatt JA, Swanson EA, et al. Optical coherence tomography of the human retina. Arch Ophthalmol 1995;113:325–32. [PubMed: 7887846]
5. Tearney GJ, Bouma BE, Fujimoto JG. High-speed phase- and group-delay scanning with a grating-based phase control delay line. Opt Lett 1997;22:1811–3. [PubMed: 18188374]
6. Wojtkowski M, Leitgeb R, Kowalczyk A, et al. In vivo human retinal imaging by Fourier domain optical coherence tomography. J Biomed Opt 2002;7:457–63. [PubMed: 12175297]
7. Leitgeb R, Hitzenberger CK, Fercher AF. Performance of Fourier domain vs. time domain optical coherence tomography. Opt Express 2003;11:889–94. [PubMed: 19461802]
8. de Boer JF, Cense B, Park BH, et al. Improved signal-to-noise ratio in spectral-domain compared with time-domain optical coherence tomography. Opt Lett 2003;28:2067–9. [PubMed: 14587817]
9. Choma MA, Sarunic MV, Yang CH, Izatt JA. Sensitivity advantage of swept source and Fourier domain optical coherence tomography. Opt Express 2003;11:2183–9. [PubMed: 19466106]
10. Srinivasan VJ, Adler DC, Chen Y, et al. Ultrahigh-speed optical coherence tomography for three-dimensional and en face imaging of the retina and optic nerve head. Invest Ophthalmol Vis Sci 2008;49:5103–10. [PubMed: 18658089]
11. Potsaid B, Gorczynska I, Srinivasan VJ, et al. Ultrahigh speed spectral/Fourier domain OCT ophthalmic imaging at 70,000 to 312,500 axial scans per second. Opt Express 2008;16:15149–69. [PubMed: 18795054]
12. Drexler W, Fujimoto JG. State-of-the-art retinal optical coherence tomography. Prog Retin Eye Res 2008;27:45–88. [PubMed: 18036865]
13. Alkuraya H, Kangave D, Abu El-Asrar AM. The correlation between optical coherence tomographic features and severity of retinopathy, macular thickness and visual acuity in diabetic macular edema. Int Ophthalmol 2005;26:93–9. [PubMed: 17063373]
14. Fujimoto H, Gomi F, Wakabayashi T, et al. Morphologic changes in acute central serous chorioretinopathy evaluated by Fourier-domain optical coherence tomography. Ophthalmology 2008;115:1494–500. [PubMed: 18394706]
15. Contreras I, Noval S, Tejedor J. Use of optical coherence tomography to measure prevalence of epiretinal membranes in patients referred for cataract surgery [in Spanish]. Arch Soc Esp Oftalmol 2008;83:89–94. [PubMed: 18260019]
16. Wilkins JR, Puliafito CA, Hee MR, et al. Characterization of epiretinal membranes using optical coherence tomography. Ophthalmology 1996;103:2142–51. [PubMed: 9003350]
17. Legarreta JE, Gregori G, Knighton RW, et al. Three-dimensional spectral-domain optical coherence tomography images of the retina in the presence of epiretinal membranes. Am J Ophthalmol 2008;145:1023–30. [PubMed: 18342830]
18. Chang LK, Fine HF, Spaide RF, et al. Ultrastructural correlation of spectral-domain optical coherence tomographic findings in vitreomacular traction syndrome. Am J Ophthalmol 2008;146:121–7. [PubMed: 18439563]
19. Forte R, Pascotto F, de Crecchio G. Visualization of vitreomacular tractions with en face optical coherence tomography. Eye 2007;21:1391–4. [PubMed: 16751756]
20. Gallemore RP, Jumper JM, McCuen BW II, et al. Diagnosis of vitreoretinal adhesions in macular disease with optical coherence tomography. Retina 2000;20:115–20. [PubMed: 10783942]
21. Ko TH, Fujimoto JG, Duker JS, et al. Comparison of ultrahigh- and standard-resolution optical coherence tomography for imaging macular hole pathology and repair. Ophthalmology 2004;111:2033–43. [PubMed: 15522369]
22. Scholda C, Wirtitsch M, Hermann B, et al. Ultrahigh resolution optical coherence tomography of macular holes. Retina 2006;26:1034–41. [PubMed: 17151491]
23. Karam EZ, Ramirez E, Arreaza PL, Morales-Stopello J. Optical coherence tomographic artefacts in diseases of the retinal pigment epithelium. Br J Ophthalmol 2007;91:1139–42. [PubMed: 17405801]
24. Keane PA, Liakopoulos S, Chang KT, et al. Comparison of the optical coherence tomographic features of choroidal neovascular membranes in pathological myopia versus age-related macular degeneration, using quantitative subanalysis. Br J Ophthalmol 2008;92:1081–5. [PubMed: 18586903]

25. Liakopoulos S, Ongchin S, Bansal A, et al. Quantitative optical coherence tomography findings in various subtypes of neovascular age-related macular degeneration. Invest Ophthalmol Vis Sci 2008;49:5048–54. [PubMed: 18566473]
26. Emerson MV, Lauer AK, Flaxel CJ, et al. Intravitreal bevacizumab (Avastin) treatment of neovascular age-related macular degeneration. Retina 2007;27:439–44. [PubMed: 17420695]
27. Ray R, Stinnett SS, Jaffe GJ. Evaluation of image artifact produced by optical coherence tomography of retinal pathology. Am J Ophthalmol 2005;139:18–29. [PubMed: 15652824]
28. Patel PJ, Chen FK, da Cruz L, Tufail A. Segmentation error in Stratus optical coherence tomography for neovascular age-related macular degeneration. Invest Ophthalmol Vis Sci 2009;50:399–404. [PubMed: 18676631]
29. Sadda SR, Wu Z, Walsh AC, et al. Errors in retinal thickness measurements obtained by optical coherence tomography. Ophthalmology 2006;113:285–93. [PubMed: 16406542]
30. Pons ME, Garcia-Valenzuela E. Redefining the limit of the outer retina in optical coherence tomography scans. Ophthalmology 2005;112:1079–85. [PubMed: 15882904]
31. Costa RA, Calucci D, Skaf M, et al. Optical coherence tomography 3: automatic delineation of the outer neural retinal boundary and its influence on retinal thickness measurements. Invest Ophthalmol Vis Sci 2004;45:2399–406. [PubMed: 15223823]
32. Chan A, Duker JS, Ko TH, et al. Normal macular thickness measurements in healthy eyes using Stratus optical coherence tomography. Arch Ophthalmol 2006;124:193–8. [PubMed: 16476888]
33. Paunescu LA, Schuman JS, Price LL, et al. Reproducibility of nerve fiber thickness, macular thickness, and optic nerve head measurements using StratusOCT. Invest Ophthalmol Vis Sci 2004;45:1716–24. [PubMed: 15161831]
34. Polito A, Del Borrello M, Isola M, et al. Repeatability and reproducibility of fast macular thickness mapping with Stratus optical coherence tomography. Arch Ophthalmol 2005;123:1330–7. [PubMed: 16219723]
35. Gurses-Ozden R, Teng C, Vessani R, et al. Macular and retinal nerve fiber layer thickness measurement reproducibility using optical coherence tomography (OCT-3). J Glaucoma 2004;13:238–44. [PubMed: 15118470]
36. Muscat S, Parks S, Kemp E, Keating D. Repeatability and reproducibility of macular thickness measurements with the Humphrey OCT system. Invest Ophthalmol Vis Sci 2002;43:490–5. [PubMed: 11818395]
37. Joeres S, Tsong JW, Updike PG, et al. Reproducibility of quantitative optical coherence tomography subanalysis in neovascular age-related macular degeneration. Invest Ophthalmol Vis Sci 2007;48:4300–7. [PubMed: 17724220]
38. Leung CK, Cheung CY, Weinreb RN, et al. Comparison of macular thickness measurements between time domain and spectral domain optical coherence tomography. Invest Ophthalmol Vis Sci 2008;49:4893–7. [PubMed: 18450592]
39. Forooghian F, Cukras C, Meyerle CB, et al. Evaluation of time domain and spectral domain optical coherence tomography in the measurement of diabetic macular edema. Invest Ophthalmol Vis Sci 2008;49:4290–6. [PubMed: 18515567]

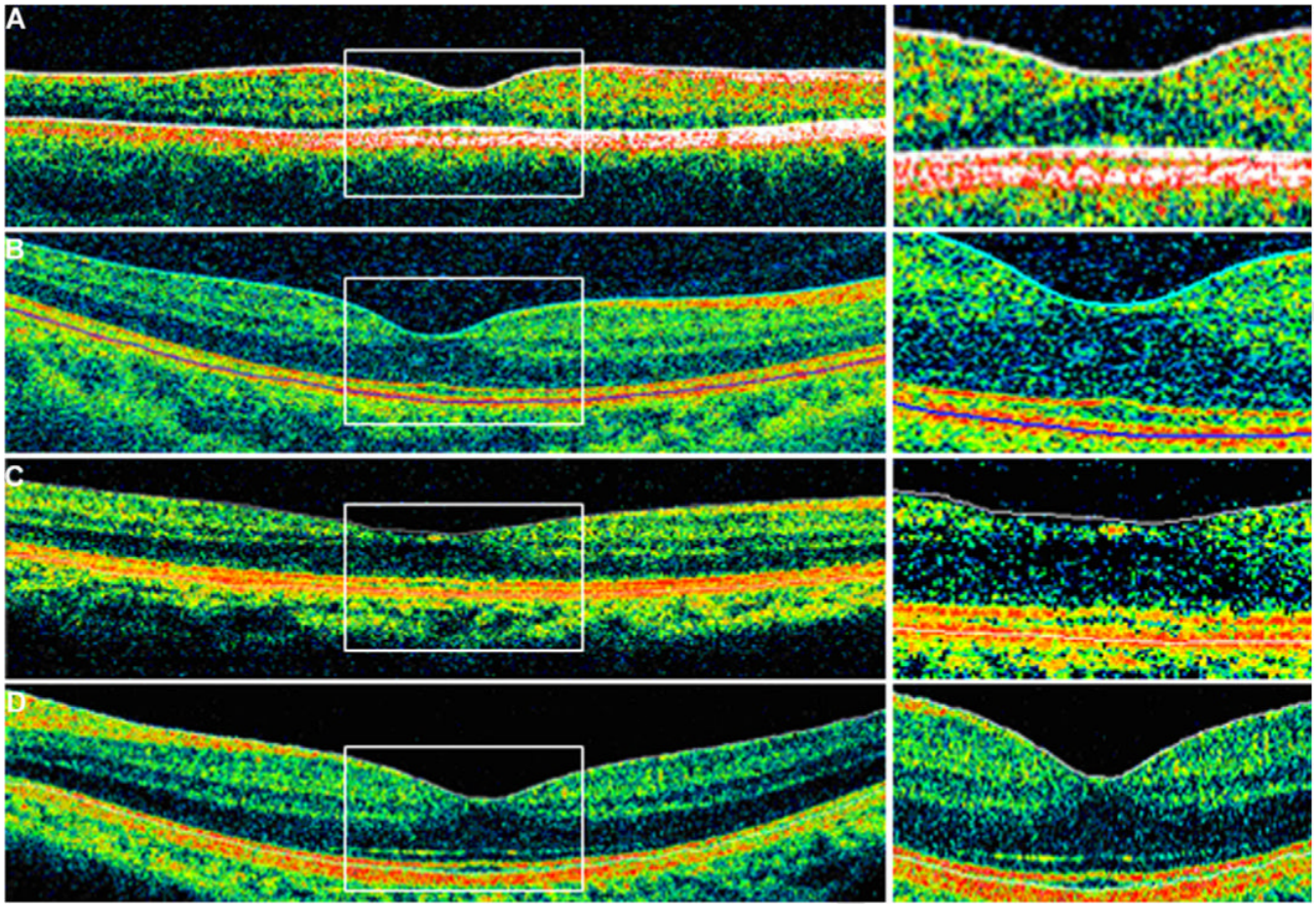

Figure 1 A-D.

Location of Optical Coherence Tomography (OCT) inner and outer retinal layer segmentation. Time domain and spectral / Fourier domain OCT all segments inner retina at the internal limiting membrane (ILM). In terms of outer retinal layer segmentation: (**A**) Stratus OCT segments at the inner segment/outer segment (IS/OS) junction,
(**B**) Cirrus HD-OCT and (**C**) RTVue-100 both segment at the retinal pigment epithelium (RPE),
(**D**) Topcon 3D OCT-1000 segments at the photoreceptor outer segment tips.

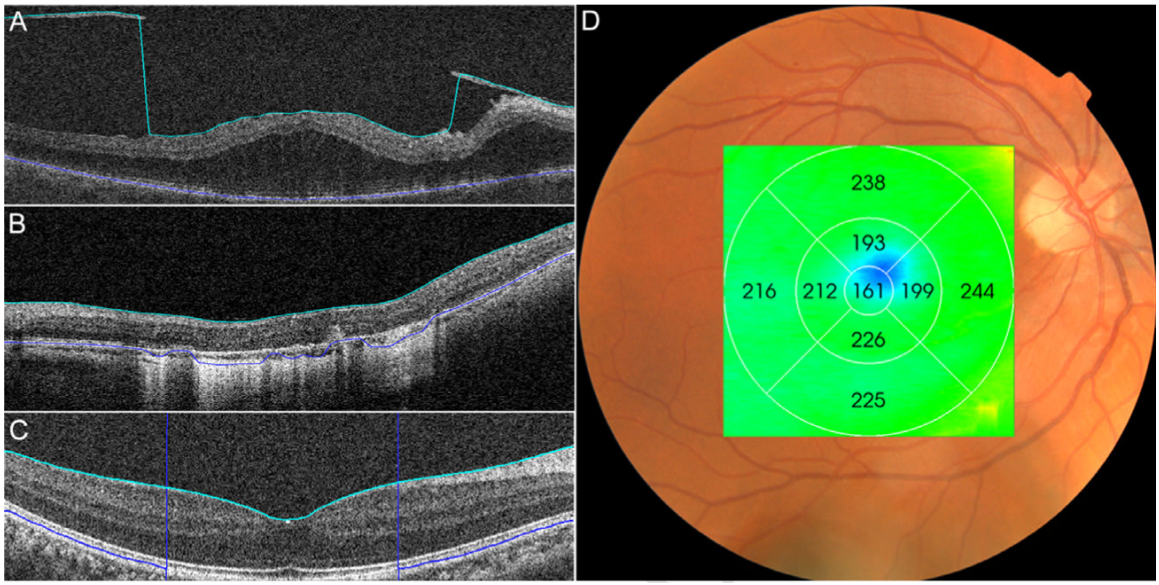

Figure 2 A-D.
Demonstration of Artifact Types:
(**A**) Inner retina misidentification: notice the light blue segmentation line followed the epiretinal membrane;
(**B**) outer retina misidentification: the dark blue segmentation line does not follow the contour of the retinal pigment epithelium (RPE);
(**C**) out of register: the RPE is shifted inferiorly thus cut out of frame causing an error in the outer retina segmentation line (in dark blue);
(**D**) off center fixation: notice the central foveal region which is delineated in blue via the topographic map is outside the central circle.

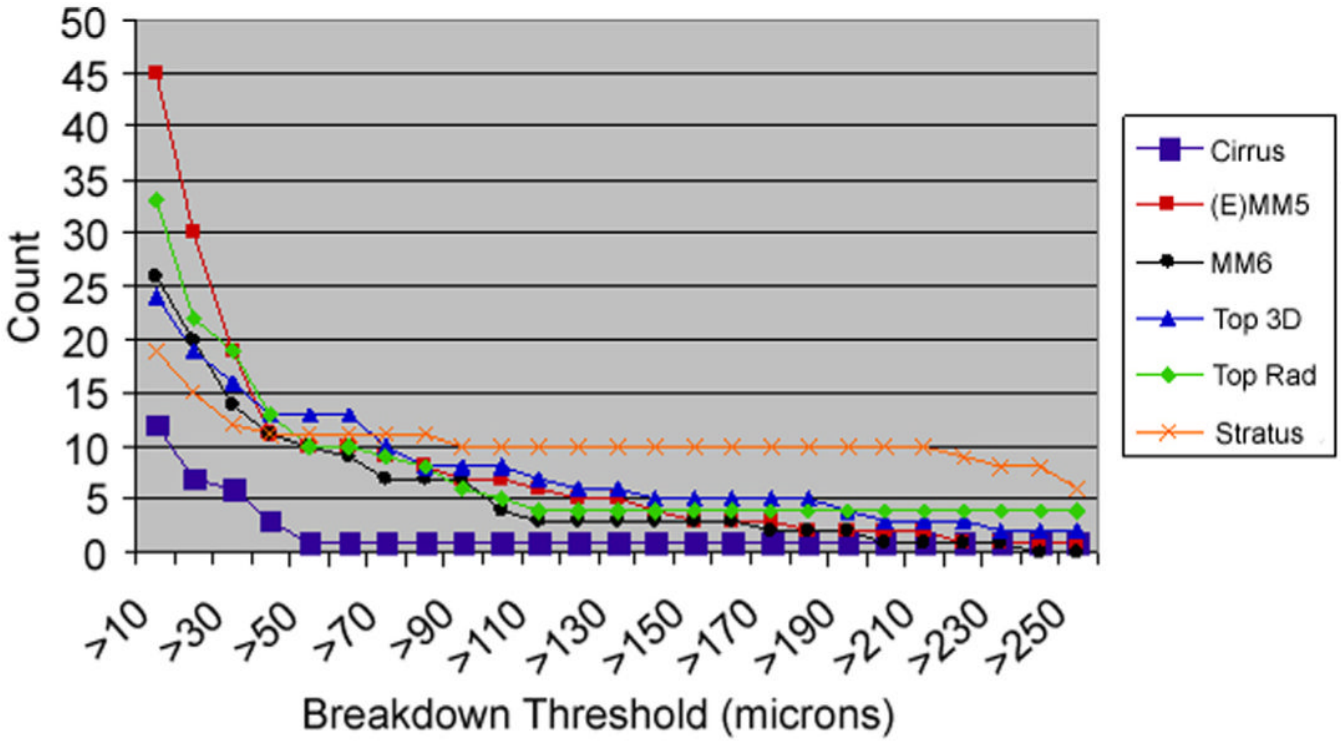

Figure 3.

Breakdown threshold graph. The absolute values of improper foveal thicknesses (in μm) are group by different thresholds of breakdown and counted for each device. Cirrus= Cirrus macular cube 512×128, (E)MM5= RTVue (E)MM5, MM6= RTVue MM6, Top 3D= Topcon 3D macular, Top Rad= Topcon Radial, Stratus= Stratus macular thickness protocol.

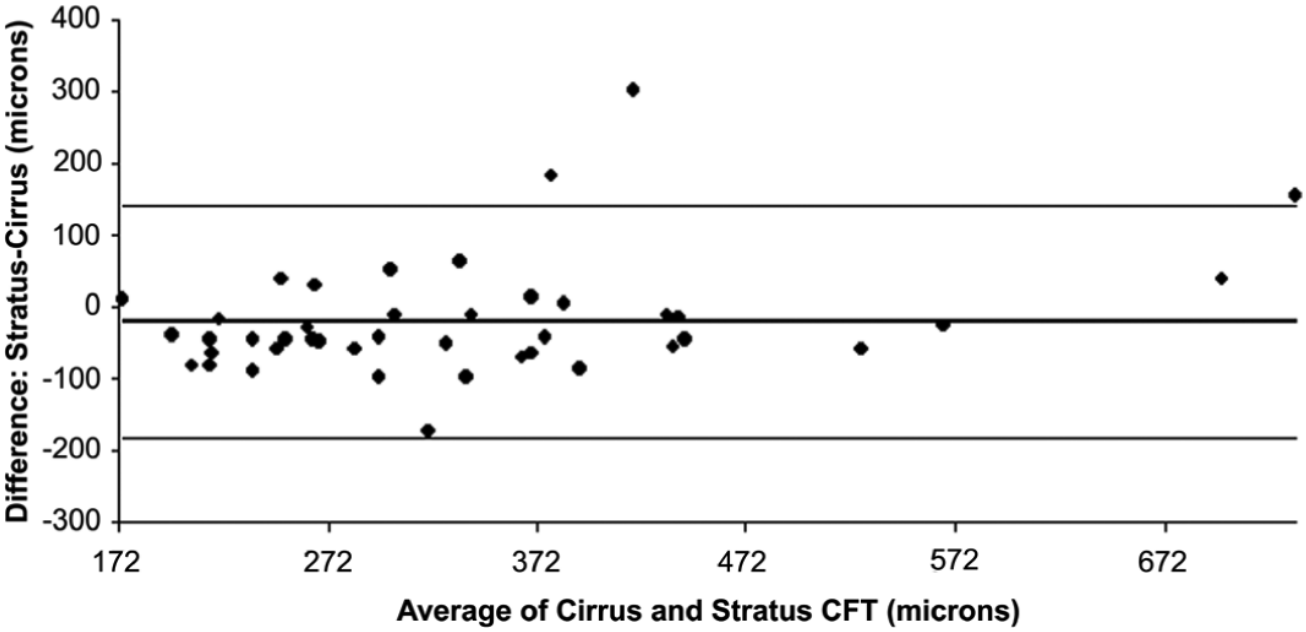

Figure 4.

Bland-Altman plot for central subfield thickness comparing Stratus OCT to Cirrus HD-OCT, shown as average of Cirrus HD-OCT and Stratus OCT (x- axis, in μm) versus the difference between thicknesses obtained from the two devices (y- axis, in μm). CFT= Central foveal thickness.

Table 1

Macular Thickness Measurements Compared.

	Stratus Macular Thickness	Cirrus Mac Cube 512×128	RTVue (E)MM5	RTVue MM6	Topcon 3D Macular	Topcon Radial	p-value
Fovea (pre-corrections)	328±144 (229, 387)	341±107 (268, 398)	359±106 (287, 430)	339±104 (262, 423)	319±116 (242, 359)	315±121 (233, 359)	<0.0001
Fovea (post-corrections)	251±195 (172, 339)	342±118 (272, 397)	352±121 (274, 401)	345±119 (266, 397)	314±125 (233, 357)	311±117 (238, 358)	<0.0001
Parafovea							
Superior	322±95 (258, 377)	343±60 (309, 368)	357±60 (314, 401)	352±66 (304, 390)	328±105 (280, 355)	321±73 (277, 355)	0.0005
Inferior	322±94 (262, 368)	345±84 (308, 390)	375±105 (313, 406)	349±61 (308, 386)	319±79 (279, 342)	324±95 (270, 360)	<0.0001
Nasal	334±106 (265, 360)	349±67 (312, 388)	367±75 (314, 396)	349±71 (303, 392)	322±70 (278, 346)	328±75 (281, 357)	<0.0001
Temporal	311±95 (253, 369)	341±70 (304, 377)	358±74 (300, 402)	347±64 (305, 370)	314±75 (262, 365)	313±80 (266, 370)	<0.0001
Perifovea							
Superior	266± 50 (230, 287)	292±39 (270, 310)	314±40 (283, 334)	293±42 (259, 313)	276±52 (243, 292)	273±54 (242, 283)	<0.0001
Inferior	253±64 (211, 272)	295±88 (258, 300)	329±98 (277, 337)	291± 41 (270, 304)	254±53 (227, 269)	274±86 (228, 300)	<0.0001
Nasal	292±90 (237, 308)	310±72 (281, 329)	334±64 (292, 345)	296±58 (264.5, 318)	289±56 (257, 300)	286±57 (250, 304)	<0.0001
Temporal	254±56 (210, 283)	288±63 (256, 301)	314±56 (277, 336)	292±41 (262, 315)	264±60 (224, 279)	259±53 (226, 285)	<0.0001

Comparison of average first-scan macular thickness measurements (in μm) across time domain and spectral / Fourier domain detection. For central foveal thicknesses, data for both pre- and post-manual corrections are presented. Average thickness ± standard deviation, along with 95% confidence interval, in parenthesis, are displayed. Significance is calculated via repeated measure analysis of variance.

Table 2

Comparison of Image Artifacts and Signal Strengths.

	Stratus Macular Thickness	Cirrus Mac Cube 512×128	RTVue (E)MM5	RTVue MM6	Topcon 3D	Topcon Radial	p-value
Any Artifacts	73.8% (31)	68.5% (37)	83.3% (45)	88.9% (48)	90.6% (48)	73.6% (39)	0.0114
IFT (Any change)	69.0% (29)	40.7% (22)	74.1% (40)	61.1% (33)	49.1% (26)	50.9% (27)	0.0031
Clinically Significant IFT (≥ 11 μm)	45.2% (19)	11.1% (6)	42.6% (23)	24.1% (13)	20.4% (11)	29.6% (16)	0.001
IRM	64.3% (27)	51.9% (28)	70.4% (38)	75.9% (41)	72.2% (39)	51.9% (28)	0.006
ORM	33.3% (14)	38.9% (21)	40.7% (22)	55.6% (30)	59.3% (32)	37% (20)	0.005
Out of Range (operator)	2.4% (1)	5.6% (3)	11.1% (6)	5.6% (3)	13% (7)	3.7% (2)	0.177
Off Center	7.1% (3)	3.7% (2)	16.7% (9)	5.6% (3)	14.8% (8)	13% (7)	0.047
Signal Strength	7.14±1.63	8.04±1.35	48.99±8.90	50.47±9.39	53.01±11.18	57.25±11.50	--

IFT= improper foveal thickness, IRM= inner retina misidentification, ORM= outer retina misidentification, p-values obtained by multiple comparison analysis of variance.

Table 3

Percent of Clinically Significant Improper Central Foveal Thickness by Disease.

	Stratus Macular Thickness	Cirrus Cube 512×128	RTVue (E)MM5	RTVue MM6	Topcon 3D Macular	Topcon Radial
ERM (15)	61.54%	10.00%	23.33%	16.67%	13.33%	26.67%
Neovascular AMD (13)	55.56%	3.85%	69.23%	19.23%	19.23%	19.23%
Non-neovascular AMD (5)	20.00%	0.00%	50.00%	10.00%	10.00%	20.00%
DME, DR (8)	20.00%	6.25%	12.5%	25.00%	12.50%	25.00%
LH/MH (4)	75.00%	12.50%	75.00%	62.50%	50.00%	62.50%
VMT (4)	66.67%	12.50%	0.00%	25.00%	0.00%	0.00%
CME (3)	0.00%	16.67%	50.00%	16.67%	0.00%	0.00%
RVO (2)	0.00%	50.00%	50.00%	50.00%	50.00%	25.00%
CSCR (3)	0.00%	16.67%	33.33%	33.33%	16.67%	33.33%
IJT (1)	0.00%	0.00%	0.00%	0.00%	0.00%	0.00%
Stargardt (1)	0.00%	0.00%	0.00%	0.00%	100.00%	50.00%
Angioid Streaks (1)	0.00%	0.00%	0.00%	0.00%	0.00%	0.00%

ERM= Epiretinal membrane, AMD= Age-related macular degeneration, DME= Diabetic macular edema, DR= Diabetic retinopathy, LH= Lamellar hole, MH= Macular hole, VMT= Vitreomacular traction, CME= Cystoid macular edema, RVO= Retinal vascular obstruction, CSCR= Central serous chorioretinopathy, IJT= Idiopathic juxtafoveal telangiectasia.

Table 4

Percentage of Inner and Outer Retina Misidentification by Disease.

	ERM (15)	N AMD (13)	DME, DR (8)	NN AMD (5)	LH/MH (4)	VMT (4)	CME (3)	CSCR (3)	RVO (2)	IJT (1)	Strg (1)	AS (1)
Outer Retina												
Stratus	20%	67%	0%	40%	25%	25%	50%	67%	0%	0%	0%	0%
Cirrus	20%	54%	38%	33%	75%	50%	67%	67%	50%	0%	0%	0%
(E)MM5	13%	60%	63%	50%	25%	50%	67%	67%	50%	0%	0%	0%
MM6	33%	77%	75%	83%	25%	50%	100%	100%	50%	0%	0%	100%
Top 3D	27%	77%	50%	83%	50%	75%	67%	100%	100%	100%	100%	0%
Top Rad	33%	23%	25%	0%	75%	50%	33%	100%	50%	0%	100%	100%
Average	24%	60%	42%	48%	46%	50%	64%	84%	50%	17%	33%	33%
Inner Retina												
Stratus	85%	56%	80%	40%	75%	67%	50%	33%	0%	0%	0%	0%
Cirrus	87%	31%	50%	33%	50%	100%	67%	33%	0%	0%	0%	0%
(E)MM5	80%	54%	50%	50%	75%	100%	67%	67%	0%	100%	0%	100%
MM6	100%	62%	67%	67%	100%	100%	100%	67%	0%	100%	0%	0%
Top 3D	100%	46%	75%	67%	75%	100%	67%	30%	50%	100%	0%	100%
Top Rad	87%	23%	63%	0%	75%	100%	67%	30%	0%	0%	0%	100%
Average	90%	45%	64%	43%	75%	95%	70%	43%	8%	50%	0%	50%

ERM= Epiretinal membrane, N AMD= Neovascular age-related macular degeneration, DME= Diabetic macular edema, DR= Diabetic retinopathy, LH= Lamellar hole, MH= Macular hole, VMT= Vitreomacular traction, NN AMD= Non-neovascular Age-related macular degeneration, CME= Cystoid macular edema, CSCR= Central serous chorioretinopathy, RVO= Retinal vascular obstruction, IJT= Idiopathic juxtafoveal telangiectasia, Strg= Stargardt disease, AS= Angioid streak, Top= Topcon, Rad= Radial.

Table 5

Bland-Altman Plot Summary.

	Central Subfield Mean ± SD	Mean Difference (Stratus-SD OCT)	Bland-Altman Limits of Agreement (95% CI)	Range (in μm)
Cirrus Mac Cube 512×128*	340±109	−12	(−184, 142)	326
RTVue (E)MM5	360±109	−32	(−193, 116)	309
RTVue MM6	339±105	−11	(−179, 140)	319
Topcon 3D	313±123	15	(−180, 180)	360
Topcon Radial	310±126	18	(−193, 203)	396

Central foveal thicknesses (μm) in Stratus OCT is compared to each spectral domain Optical Coherence Tomography device. Bland-Altman limits of agreement and range of 95% confidence interval are also displayed (both in μm). SD= standard deviation, CI= confidence interval.

*Example of Bland-Altman plot is shown in Figure 4.

Table 6

Reproducibility of First to Second Scan Macular Thickness Measurements.

	Cirrus Mac Cube 512×128			RTVue (E)MM5			RTVue MM6			Topcon 3D			Topcon Radial		
	ICC	95% CI		ICC	95% CI		ICC	95% CI		ICC	95% CI		ICC	95% CI	
		Low	High		Low	High		Low	High		Low	High		Low	High
Fovea	0.92	0.86	0.95	0.92	0.87	0.95	0.95	0.91	0.97	0.96	0.92	0.97	0.97	0.95	0.98
Parafoveal															
Superior	0.93	0.89	0.96	0.83	0.72	0.90	0.93	0.88	0.96	0.21	−0.06	0.45	0.96	0.94	0.98
Inferior	0.84	0.73	0.90	0.93	0.88	0.96	0.84	0.75	0.91	0.43	0.19	0.62	0.89	0.81	0.93
Nasal	0.93	0.89	0.96	0.88	0.81	0.93	0.82	0.70	0.89	0.95	0.91	0.97	0.99	0.98	0.99
Temporal	0.73	0.58	0.83	0.89	0.82	0.94	0.80	0.68	0.88	0.94	0.89	0.96	0.90	0.83	0.94
Perifoveal															
Superior	0.95	0.92	0.97	0.88	0.80	0.93	0.24	−0.03	0.47	0.87	0.79	0.92	0.94	0.90	0.96
Inferior	0.69	0.52	0.80	0.86	0.77	0.91	0.69	0.52	0.81	0.54	0.31	0.71	0.76	0.61	0.85
Nasal	0.95	0.92	0.97	0.78	0.65	0.87	0.80	0.68	0.88	0.96	0.94	0.98	0.85	0.75	0.91
Temporal	0.62	0.42	0.76	0.82	0.71	0.89	0.75	0.61	0.85	0.89	0.82	0.93	0.49	0.26	0.67

ICC= intraclass correlation coefficient, CI= confidence interval.